

**University of Massachusetts Amherst**  
**ScholarWorks@UMass Amherst**

---

Computer Science Department Faculty Publication  
Series

Computer Science

---

1998

# Feature Detection and Identification using a Sonar-Array

E. G. Araujo

*University of Massachusetts Amherst*

Follow this and additional works at: [https://scholarworks.umass.edu/cs\\_faculty\\_pubs](https://scholarworks.umass.edu/cs_faculty_pubs)



Part of the [Computer Sciences Commons](#)

---

## Recommended Citation

Araujo, E. G., "Feature Detection and Identification using a Sonar-Array" (1998). *Computer Science Department Faculty Publication Series*. 86.

Retrieved from [https://scholarworks.umass.edu/cs\\_faculty\\_pubs/86](https://scholarworks.umass.edu/cs_faculty_pubs/86)

This Article is brought to you for free and open access by the Computer Science at ScholarWorks@UMass Amherst. It has been accepted for inclusion in Computer Science Department Faculty Publication Series by an authorized administrator of ScholarWorks@UMass Amherst. For more information, please contact [scholarworks@library.umass.edu](mailto:scholarworks@library.umass.edu).

## Feature Detection and Identification using a Sonar-Array\*

E. G. Araujo

R. A. Grupen

Laboratory for Perceptual Robotics<sup>†</sup> - Department of Computer Science

University of Massachusetts, Amherst MA 01003 USA

e-mail: {araujo, grupen}@cs.umass.edu

### Abstract

*This work explores techniques for sonar sensor fusion in the context of environmental feature detection and identification for navigation tasks. By detecting common features in indoor environments and using them as landmarks, a robot can navigate reliably, recovering its pose when necessary. Preliminary results on a multiple hypothesis testing procedure for feature localization and identification show that accurate feature information can be acquired with adequate sonar models and configurations. In addition, a method that associates sonar configuration with the precision of feature extraction is discussed, as well as its utility for guiding an active sonar sensor.*

## 1 Introduction

Sound-based navigation has been shown to be effective, not only in man-made systems, but primarily in nature. Bats master echolocation [13], suggesting that sonars can extract high level information from the environment.

This paper is focused on the extraction of specific information from the environment to reduce pose uncertainty in robot navigation tasks. We envision circumstances when geometric models of the environment are not available, or are unreliable due to odometry errors. The objective is to identify feature sets which actively resolve localization errors. Section 2 introduces sonar models and configurations, followed by the description of the sensor system selected in Section 3. Sections 4 and 5 present the feature localization models, a method to estimate feature errors, and a multiple hypothesis testing method for feature localization and identification. The experiments are discussed in Section 6, and Section 7 concludes the paper.

## 2 Sonar Sensor

In this paper, sonar represents airborne ultrasonic range sensing based uniquely in time-of-flight (TOF). The main

advantages of using sonars in mobile robots are their low price, range of actuation, simple interface, and typically accurate readings. However, the response time of sonars is limited by the velocity of sound in air, multiple simultaneous sonar firings may cross-talk, and multi-target reflections are difficult to model, normally causing inconsistencies between some of the readings (in some cases more than 50%) and the model used. These limitations make the use of sonar a challenge to sensor modeling, data fusion, and sensor management, creating a fertile testbed for addressing the problem of reasoning with uncertainty.

### 2.1 Sonar-Based Modeling

Sonar-based modeling in the literature belongs to two main classes: grid-based probabilistic models that avoid direct modeling of the environment [6, 3, 7], and feature-based models that exploit the interaction between sonar beam and frequently encountered environmental features [5, 9, 10, 8]. Complementing these methods, sensor fusion approaches and data pre-filtering algorithms are widely used, not only to reduce uncertainty, but also to identify contexts consistent with the model employed.

One of the first models presented was a feature-based model [5], where surface information is extracted from raw sonar data, and applied to map building. Limitations of this approach led to the use of grid-based probabilistic models, such as occupancy grids and vector fields [6, 3]. The argument used in favor of a probabilistic approach to modeling is that raw sonar data is subject to several, difficult to model, environmentally dependent effects such as specular reflections and sensor cross-talk, and thus geometrical reasoning purely on the basis of raw data is not appropriate.

Some authors considered a specular reflection to occur when the difference between wavefront incident angle and the normal to a smooth surface is too large, causing no return signal. In this case, objects are assumed to be detected mainly by diffuse reflectance [5, 6, 3]. Subsequent feature-based models were developed based-on a specular reflectance model. They argued that indoor environments consist mainly of *specular* surfaces, based on the significantly different acoustic impedances of air and solids, and the wavelength of ultrasound compared to object surface roughness [10]. Specular world assumptions proved to be

\*This work was supported by NSF under IRI-9503687, IRI-9704530, and CDA-9703217.

<sup>†</sup><http://piglet.cs.umass.edu:4321>

more general and allowed a detailed geometric analysis of the interaction between sonar beam and common office environment. This fact gave a new spin to the use of feature-based sonar models, showing that even simple sonar devices could produce better quality information when used with an adequate model and sensor configuration [10, 12].

There is no best approach to sensor configuration or modeling. In general, they are task and environment dependent. For example, obstacle avoidance tasks favor a grid-based model, a sonar ring configuration, and multiple simultaneous transmitters since this design deals, to some extent, with dynamic environments. On the other hand, a pose localization task requires more precise information about common and consistent features in the environment (landmarks), and thus favors a feature-based model applied to an array of sonars with multiple receivers.

## 2.2 Sonar Configurations

Methods to extract information from sonar are highly dependent on sonar configuration – the geometric relationship between transmitters, reflective features, and receivers. Robots normally come with transducers evenly distributed around their periphery in a plane parallel to the floor; rings with 8 to 24 sonars are common. This configuration facilitates obstacle avoidance, because multiple sonars can quickly observe the robot’s surroundings. However, since the overlap between sonar beams is minimal, performance on tasks such as tracking and pose localization is compromised. Solutions to these tasks usually employ localized, densely sampled data, obtained from a rotating transducer, or array of transducers [10, 12, 11, 4]. Only recently, the utility of different sonar configurations has been studied with the introduction of sonar arrays – groups of transducers that collaborate on a measurement [11, 8, 4, 1].

## 3 Sonar System

The study conducted evaluates the performance of feature detection as sonar configuration varies. The idea is to detect a set of common features in indoor environments and to use these features as landmarks (anchors), allowing the robot to navigate reliably, by keeping, or recovering its pose when necessary. The general applicability of this method depends not only on the accuracy of the sensor model and the sensor configuration selected, but also on how detectable the features selected are. The environmental features selected are those used by Kuc in [9], representing walls, concave, and convex room features. These indoor features have the characteristics required above, and closed-form solutions for their detection in specular environments exist for some sonar configurations [11, 8].

Three sensor configurations, depicted in Figure 1, were considered: a sonar ring with 24 sonars, a rotating sonar

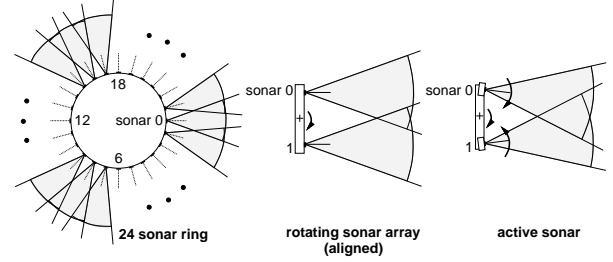


Figure 1. Sonar spatial configurations.

array with aligned transducers, and an active sonar array where each sonar has an extra DOF (pan). The sonar ring executes at most 3 simultaneous transmissions from transducers evenly separated to minimize cross-talk, and uses the entire ring as receiver. The second configuration employs a rotating 2-sonar array with one sonar transmitting and all receiving. The impact of these configurations on feature detection and identification is reported in Section 6.

## 4 Feature Detection

The goal of extracting features from the environment is to use them as landmarks, or anchors in navigation tasks. The feature set selected represents the characteristic sonar responses of individual planes and conjunctions of planes – both convex and concave. We refer to these features as lines, edges, and corners. The assumption of a specular environment is imperative to the feature model derivation, and was shown not to be restrictive in practice [9, 8].

### 4.1 Feature Localization Models

The feature models described here use range information from a pair of return signals derived from TOF, under the assumption that the velocity of sound is constant ( $\approx 343 \text{ m/s}$ ). In a sonar pair, one transducer operates as transmitter and receiver ( $T$ ), returning the range  $r_1$ , and the other operates as receiver only ( $R$ ), producing  $r_2$ . The range pair  $(r_1, r_2)$  is used then to compute a position estimate for each feature type, assuming that both readings come from the same feature.

**4.1.1 Line Feature.** The line feature model uses the pair of ranges  $(r_1, r_2)$  and the position and orientation estimate of the transducer  $T (x_T, y_T, \phi_T)$  to create a line position estimate  $(r, \theta)$ . Figure 2 shows the reflections generated by the ultrasonic signal on a planar reflector, where  $T'$  and  $R'$  are virtual images of  $T$  and  $R$ , respectively. Under these circumstances,  $(r_1, r_2)$  must satisfy the following relations:

$$r_2 = \sqrt{r_1^2 - 2r_1d \sin(\alpha) + d^2} \quad (1)$$

$$\alpha = \arcsin \left( \frac{d^2 + r_1^2 - r_2^2}{2dr_1} \right) \quad (2)$$

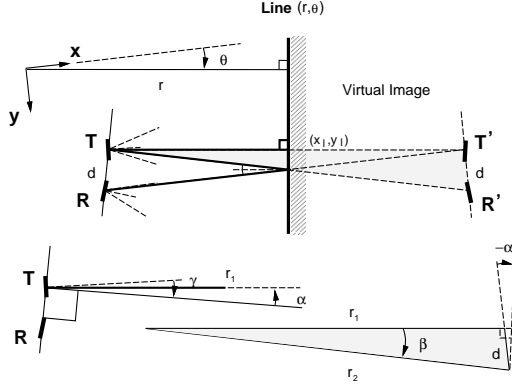


Figure 2. Line reflection.

where  $d$  is the distance between transducers,  $\alpha$  is the angle between the line connecting the transducers and the feature, and  $\beta$  is the angle between sonar bearings of  $r_1$  and  $r_2$ .

The line parameters  $(r, \theta)$  are computed given the angle  $\alpha$  from Equation 2 and the angle  $(\gamma)$  between the transducer  $T$  orientation and the normal to the line that connects the transducers, as depicted in Figure 2:

$$r = x_l \cos(\theta) + y_l \sin(\theta), \quad \theta = \phi_T + \xi$$

where:

$$\xi = \gamma + \alpha$$

$$x_l = x_T + \frac{r_1}{2} \cos(\phi_T + \xi) \quad (3)$$

$$y_l = y_T + \frac{r_1}{2} \sin(\phi_T + \xi) \quad (4)$$

**4.1.2 Corner Feature.** The corner feature, composed of two intersecting orthogonal specular planar surfaces, uses the range pair and the current position and orientation estimate of the transducer  $T$  to create the corner position estimate  $(x_c, y_c)$ . The reflection of the ultrasonic signal on a corner feature is shown in Figure 3, where the relation between sonar ranges are the same as the line feature (Equations 1 and 2), except for an inverse sign on the angle  $\beta$ , and that  $\alpha$  here represents the angle between the line that connects the transducers and the corner feature. The corner parameters  $(x_c, y_c)$  are also identical to the line feature parameters (Equations 3 and 4), anticipating that these features cannot be distinguished from a single sonar position.

**4.1.3 Edge Feature.** The edge feature model also uses the pair of sonar ranges and the current position and orientation estimate of the transducer  $T$  to create the edge position estimate  $(x_e, y_e)$ . But the assumptions required for modeling an edge feature are distinct; the point of reflection is assumed to be independent of the sonars position, and the edge must be a high curvature<sup>1</sup> convex corner. The reflections from a sharp edge is modeled as pure diffusion, and

<sup>1</sup>Radius smaller than the wavelength of the sonar signal,  $\psi < 7mm$ .

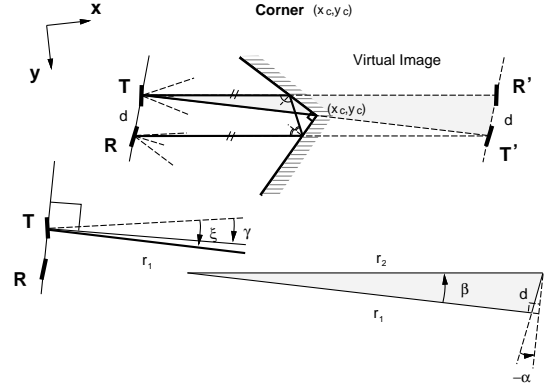


Figure 3. Corner reflection.

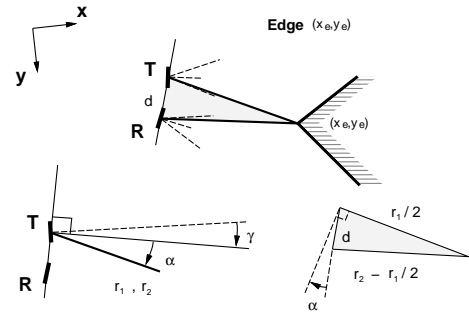


Figure 4. Edge reflection.

not specular reflection as on the other features. Figure 4 shows typical reflections on an edge, where these relations are extracted:

$$r_2 = \frac{r_1}{2} + \sqrt{\left(\frac{r_1}{2}\right)^2 + d^2 - r_1 d \sin(\alpha)}$$

$$\alpha = \arcsin\left(\frac{d^2 + r_1 r_2 - r_2^2}{dr_1}\right) \quad (5)$$

where  $\alpha$  is the angle between the line that connects the transducers and the edge feature. Notice that  $\beta$ , the angle between sonar bearings corresponding to  $r_1$  and  $r_2$ , is zero. The derivation of the edge parameters  $(x_e, y_e)$ , similarly to the previous features, uses the angle  $\alpha$  from Equation 5, and is given by Equations 3 and 4.

## 4.2 Feature Localization Error

To complete the derivation of the feature localization models, it is necessary to estimate the uncertainty associated with each feature parameter, using: the sonar measurements' uncertainty  $(\Delta r_1, \Delta r_2)$ , the non-linear transformations from measurement to feature space, and the transducers configuration together with their beam angle estimates.

The method presented computes the error in feature space by means of geometric analysis, estimating the region in space that might contain the feature true position.

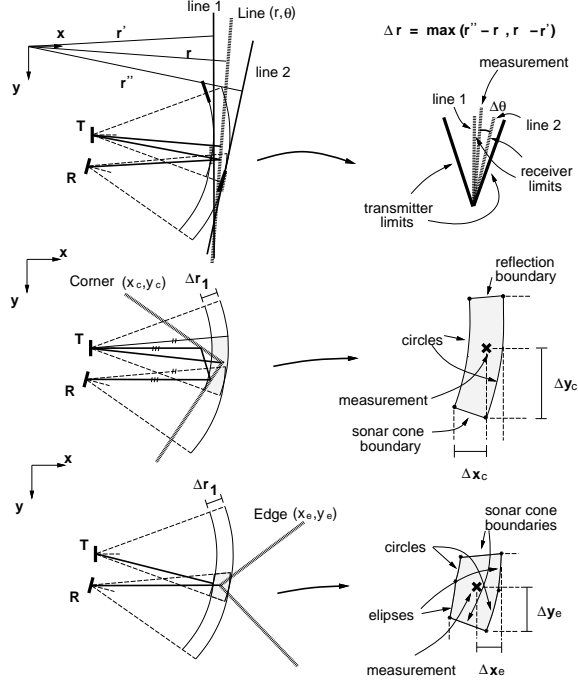


Figure 5. Feature localization error.

The uncertainty in the feature localization can then be calculated indirectly from the resulting estimation, as depicted in Figure 5. The algorithm below summarizes the method.

**Feature Error Calculation (Geometric Method):**

1. Given the sonar measurements ( $r_1 \pm \Delta r_1$ ,  $r_2 \pm \Delta r_2$ ), the sonar configuration, the beam angles, and the type of feature under analysis, calculate the region where the sonar reflections could occur.
2. Return the error in the feature localization ( $\Delta x, \Delta y, \Delta r$ , or  $\Delta \theta$ ) given the above region. If such region does not exist, ignore the measurement.

The main advantage of this approach is the direct association between sensor configuration and precision on the measurement. In measurement space, the error associated with the measurements is directly proportional to the measurements' value; therefore, to obtain a more precise measurement, the sensors should get closer to the object being measured. In feature space, not only the sensors distance to a feature but also the configuration of the sensors and the feature type play an important role on feature error minimization and on feature characterization. Some techniques used in radar systems that actively exploits the configuration of two antennas to improve measurement quality can also be applied here to the sonar system [14].

In the case of an edge or line feature, a more precise measurement is obtained when the overlap between the receiver and transmitter cones is minimized by rotating the

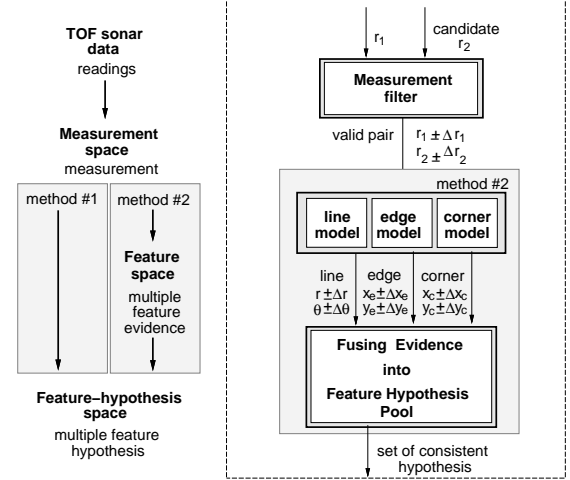


Figure 6. Feature localization procedure.

transducers, or by increasing their distance ( $d$ ). This is also true for the corner feature, except that the receiver and transmitter cones do not need to overlap, since the error region is produced by the reflection boundary, and not by the receiver cone boundary [1]. All these facts can be exploited on the design of active sonar sensor controllers.

### 4.3 Feature Localization Procedure

Figure 6 depicts the process of extracting feature localization hypotheses from raw sonar data. The sonar raw information is pre-filtered yielding consistent sonar measurement pairs. Then each pair is transformed into a feature localization using the feature models. Over time, feature evidence from independent observations are fused [2]. The first method (Method #1) uses extended Kalman Filters, converting from measurement space to feature-hypothesis automatically. Method #2 first transforms a measurement into supporting evidence for all three features (line, edge, and corner), and then uses linear Kalman Filters to incorporate the feature evidence into the feature hypothesis pool. This paper uses Method #2, and the derivation of the Kalman filters for both methods can be found in [1].

To discard a measurement with readings from different features, a pre-filter based on relations derived from the feature models was used (Measurement Filter). Equations 2 and 5 express those relations that evaluate to the constraint (Eq. 6) since  $r_1$ ,  $r_2$ , and  $d$  are positive and  $r_1 > d$ ; eliminating to some extent readings that are not consistent with the feature models employed.

$$\left| \frac{d^2 + r_1^2 - r_2^2}{2dr_1} \right| \leq 1, \quad \left| \frac{d^2 + r_1r_2 - r_2^2}{dr_1} \right| \leq 1$$

$$|r_2 - r_1| \leq d \quad (6)$$

Information is ultimately expressed in the form of multiple feature observations, each composed of a line ( $r \pm \Delta r$ ,  $\theta \pm \Delta \theta$ ), edge ( $x_e \pm \Delta x_e$ ,  $y_e \pm \Delta y_e$ ), and corner hypotheses ( $x_c \pm \Delta x_c$ ,  $y_c \pm \Delta y_c$ ). These observations are then fused into the feature hypothesis pool, where each hypothesis keeps a Kalman filter running for each feature type.

In updating the feature-hypothesis pool, the problem of verifying whether a new observation belongs to an existing feature-hypothesis in the pool has to be addressed. The metric used, as shown on the procedure below, computes the probability that a sample could be drawn from both Gaussian distributions (evidence and hypothesis). The metric assumes values between 0 and 1, and is 1 when the distributions are identical, and zero when there is no overlap between them (both distributions were truncated at  $\pm 3\sigma$ ).

---

*Selecting in which hypothesis to fuse the new observation:*

1. Compute the similarity metric for each feature-hypothesis in the pool of hypotheses, and for each feature type;
  2. Search for the hypothesis that has the higher metric value;
  3. Return the hypothesis' id if its metric value exceeded a threshold ( $thr = 0.3$ ); otherwise create a new hypothesis.
- 

## 5 Feature Identification

The last step is to identify the feature type which best accounts for the data. Our approach calculates a confidence measurement for each feature of a hypothesis with variance  $\sigma^2 < 0.001$ , and selects a feature that has a significantly higher value, as described in the following algorithm.

---

*Feature confidence measurement:*

1. On the last  $n$  measurements ( $n \leq 20$ ) fused into the hypothesis, use their corresponding sonar configurations to:
    - (a) Compute which sonar measurements the current filter feature estimate generates;
    - (b) Compare the above measurements with the original measurements fused, by using the same metric used to select in which hypothesis to fuse a new evidence;
  2. Compute each feature confidence by taking the average of all the metric values over the  $n$  measurements;
  3. Select the feature with the best confidence value, higher (0.2) than the second best on this hypothesis.
- 

The feature identification process requires information from multiple sonar configurations and sometimes even different robot poses to correctly distinguish between features. Thus, the acquisition of information must be done actively, based on previous knowledge of how and where relevant information can be obtained.

## 6 Experiments

A 2D simulator was developed for testing sonar configurations in specular environments composed of lines, edges, and corners. The simulator uses the feature models, a simple model of the ultrasonic sensor that considers range and beam angle (0.3 to 10 m, and  $40^\circ$ ), and a Gaussian noise process to corrupt the sonar returns (at most 1% error). Thus, the idea is not to test the robustness of the method with respect to uncertainty in the feature models, but to identify configurations that facilitate the extraction of features to be used as navigational feedback.

Figure 7 depicts an experiment designed to test the performance of a rotating 2-sonar array and a 24 sonar ring. The environment selected is composed of 12 features (lines, corners, and an edge), approximately 6 by 3 m, and the sonar apparatus is located 2 m from the left-side wall and 1 m from the top wall. The left and middle simulator snapshots, taken after 3 full scans ( $\approx 300$  firings), show all the hypotheses created (represented by crosses). The middle snapshot shows the 5 features correctly identified by the system (crosses), together with the raw data used (dots). The absolute localization error of the features extracted on each sonar scan is reported in Table 1, where the localization error is on average one order of magnitude better than the uncertainty of the raw data. The last snapshot presents all the hypotheses created by a ring after the same amount of firings, but, in this case, no feature was identified.

Scan #			1	2	3	4
Total # of features identified			2	4	5	5
Total # of hypothesis			9	9	9	9
Absolute feature error $r, x, y$ in m $\theta$ in rad	Top wall	$r$	0.002	0.002	0.001	0.000
		$\theta$	0.001	0.002	0.000	0.000
	Bottom wall	$r$	—	0.010	0.007	0.008
		$\theta$	—	0.006	0.004	0.005
	Left-side wall	$r$	0.008	0.003	0.001	0.011
		$\theta$	0.006	0.001	0.000	0.010
	Left-upper corner	$x$	—	0.001	0.006	0.002
		$y$	—	0.012	0.019	0.010
	Left-lower corner	$x$	—	—	0.017	0.008
		$y$	—	—	0.007	0.005

Table 1. Feature extraction results from 2-sonar array.

Both configurations have advantages and drawbacks. As demonstrated, the 2-sonar array not only detected more features than the ring, but also correctly identified all the nearby features. On the other hand, the ring was able to localize 4 out of 5 features faster than the 2-sonar array, and it is an effective configuration for obstacle avoidance. In a navigation task a synergetic relation can be created where a sonar ring can contribute by directing a rotating sonar array to places with high probability of finding a landmark, navigating reliably and avoiding obstacles.

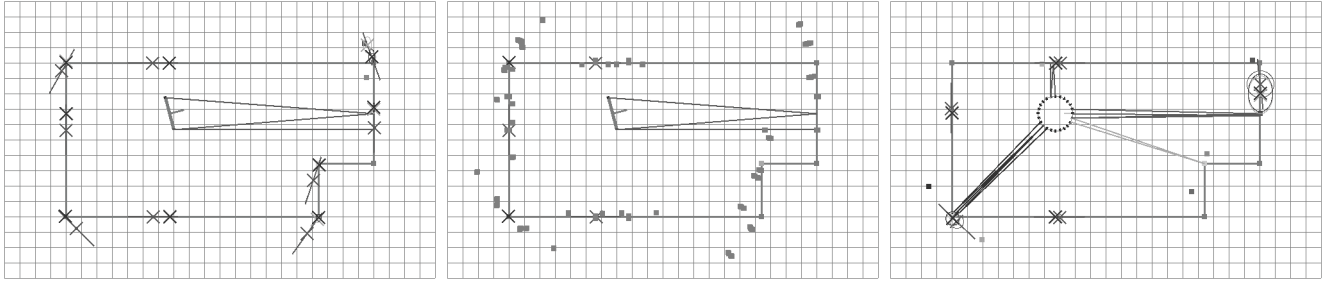


Figure 7. Simulator snapshots of a rotating 2-sonar array (left, middle) and a 24 sonar ring (right).

## 7 Conclusions and Future Work

This paper presents a procedure based on multiple hypothesis testing for localizing and identifying indoor features using sonar data, demonstrating that accurate feature information can be acquired with the use of an adequate sonar model and configuration. The geometric method presented for feature error calculation showed a direct association between sensor configuration and localization precision, suggesting the possibility of creating sonar controllers capable of extracting better information by actively exploiting sensor configuration.

The sonar system of our mobile robot is currently being modified, and an active sonar sensor is being developed to further validate the results presented in this paper. Figure 8 shows our mobile robot and the stereo-head system where the active sonar will be tested. The transducers can be seen mounted above the cameras.

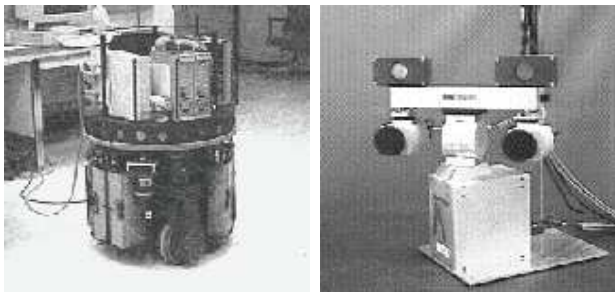


Figure 8. Mobile robot and proposed active sonar.

## References

- [1] E. G. Araujo and R. A. Grupen. Feature extraction for autonomous navigation. Tech. Rept. 97-55, Dept. of Comp. Sci., Univ. of Massachusetts, Amherst, 1997.
- [2] Y. Bar-Shalom and T. E. Fortmann. *Tracking and Data Association*, Vol. 179 of *Math. Sc. Eng.*. Academic Press, Inc., 1989.
- [3] J. Borenstein and Y. Koren. The vector field histogram - fast obstacle avoidance for mobile robots. *IEEE Trans. Robot. Automat.*, 7(3):278–288, 1991.
- [4] K. S. Chong and L. Kleeman. Indoor exploration using a sonar sensor array: A dual representation strategy. In *IEEE Proc. IROS*, Vol. 2, pp. 676–682, Grenoble, France, Sept. 1997.
- [5] J. L. Crowley. Dynamic world modeling for an intelligent mobile robot using a rotating ultra-sonic ranging device. In *Proc. IEEE Int. Conf. Robot. Automat.*, Vol. 1, pp. 128–135, St. Louis, MO, Mar. 1985.
- [6] A. Elfes. Sonar-based real-world mapping and navigation. *IEEE J. Robot. Automat.*, RA-3(3):249–265, June 1987.
- [7] A. Elfes. Dynamic control of robot perception using multi-property inference grids. In *Proc. IEEE Int. Conf. Robot. Automat.*, Vol. 3, pp. 2561–2567, Nice, France, May 1992.
- [8] L. Kleeman and R. Kuc. Mobile robot sonar for target localization and classification. *Int. J. Robot. Res.*, 14(4):295–318, Aug. 1995.
- [9] R. Kuc and M. W. Siegel. Physically based simulation model for acoustic sensor robot navigation. *IEEE Trans. Pattern Anal. Mach. Intell.*, PAMI-9(6):766–778, Nov. 1987.
- [10] J. J. Leonard and H. F. Durrant-Whyte. *Direct Sonar Sensing for Mobile Robot Navigation*, Vol. SECS 175 of *The Kluwer Int. Series in Eng. and Comp. Sci.*. Kluwer Academic Publishers, Norwell, MA, 1992.
- [11] J. Manyika and H. F. Durrant-Whyte. *Data Fusion and Sensor Management: A Decentralized Information-Theoretic Approach*. Ellis Horwood Series in Electrical and Electronic Engineering, 1994.
- [12] H. Peremans and J. Van Campenhout. Tri-aural perception on a mobile robot. In *Proc. IEEE Int. Conf. Robot. Automat.*, Vol. 1, pp. 265–270, Atlanta, GA, May 1993.
- [13] J. A. Simmons and A. D. Grinnell. The performance of echolocation: Acoustic images perceived by echolocating bats. In P. E. Nachtigall and P. W. B. Moore, editors, *Animal Sonar: processes and Performance*, Vol. 156 of *NATO ASI Series. Series A. Life Sciences*, pp. 353–385. Plenum Press, 1988.
- [14] M. I. Skolnik. *Introduction to radar systems*. McGraw-Hill, New York, 1962.